Water vapour variability in the high-latitude upper troposphere: 2. Impact of volcanic emissions

C. E. Sioris[1], J. Zou[2], C. T. McElroy[1], C. D. Boone[3], P. E. Sheese[2], and P. F. Bernath[3,4]

[1] {Department of Earth and Space Science and Engineering, York University, Toronto, Canada, 4700 Keele St., Toronto, ON, Canada, M3J 1P3}

[2] {Department of Physics, University of Toronto, 60 St. George. St., Toronto, ON, Canada, M5S 1A7}

[3] {Department of Chemistry, University of Waterloo, 200 University Ave. W, Waterloo, ON, Canada, N2L 3G1}

[4] {Department of Chemistry & Biochemistry, Old Dominion University, 4541 Hampton Blvd., Norfolk, VA, USA, 23529}

Correspondence to: C. E. Sioris (csioris@sdcnlab.esse.yorku.ca)

Abstract

The impact of volcanic eruptions on water vapour in the high latitude upper troposphere is studied using deseasonalized time series based on observations by the Atmospheric Chemistry Experiment (ACE) water vapour sensors, namely MAESTRO (Measurements of Aerosol Extinction in the Stratosphere and Troposphere Retrieved by Occultation) and the Fourier Transform Spectrometer (ACE-FTS). The two eruptions with the greatest impact on the high latitude upper troposphere during the time frame of this satellite-based remote sensing mission are chosen. The Puyehue-Cordón Caulle volcanic eruption in June 2011 was the most explosive eruption in the past 24 years and resulted in an observed (50±12)% increase in water vapour in the southern high-latitude upper troposphere in July 2011 that persisted into September 2011. Eyjafjallajökull erupted in 2010, increasing water vapour in the upper troposphere at northern high latitudes significantly for a period of ~1 month. These findings imply that volcanogenic steam emitted or transported to the high-latitude upper troposphere must be taken into account to properly determine the magnitude of the local trend in water vapour over the last decade.

1 Introduction

Water vapour in the tropopause region is particularly effective at trapping outgoing longwave radiation emitted by the surface (Solomon et al., 2010). Currently, trends in UTWV are not known for high latitudes (Hartmann et al., 2013). The first step toward accurate trends is to improve our understanding of UTWV variability at high latitudes. The variability of upper tropospheric water vapour (UTWV) at high latitudes is dominated by dynamics (Sioris et al., 2015). In this companion paper, a second phenomenon is identified that contributes secondarily to the variability of UTWV: volcanic emissions. The role of volcanic emissions relative to other dynamical and thermodynamic processes in this region on monthly timescales is an open question which motivates this study. Water vapour is the most abundant volcanic gas, comprising over 80% by volume (Pinto et al., 1989). UTWV was observed to decrease following the Pinatubo eruption due to global cooling below the tropopause and did not return to normal levels for two years (Soden et al., 2002). For volcanoes with an eruption height at or below tropopause, local warming by radiation-absorbing volcanic aerosols such as ash can lead to local increases in water vapour. The timescale of UTWV enhancement due to such a thermal mechanism would be controlled by rainout and fallout of the aerosol, which is on the order of ~1 month (Prospero, 1983; Pruppacher and Klett, 2010) for particles of intermediate size (~0.3 μm). Water vapour at the tropopause has a typical atmospheric residence time on the order of three weeks (Ehhalt, 1973; Brasseur et al., 1998) and is mostly removed by precipitation (Junge, 1963). The residence time decreases to ~2 weeks at an altitude of 5 km (Ehhalt, 1973) which limits the distance over which UTWV enhancements can be advected.

Two recent volcanic eruptions which produced the most obvious upper tropospheric water vapour enhancements at high latitudes, namely Puyehue Cordón Caulle (June 2011) and Eyjafjallajökull (April 2010), are studied here using satellite-based observations.

2 Methods

SCISAT was launched in 2003 (Bernath et al., 2005) and the Atmospheric Chemistry Experiment (ACE) datasets begin in February 2004. The satellite bears two limb sounders measuring water vapour that both rely on the solar occultation technique: Measurements of Aerosol Extinction in the Stratosphere and Troposphere Retrieved by Occultation (MAESTRO, McElroy et al., 2007) and the Fourier Transform Spectrometer (ACE-FTS) as well as an Imager (Bernath et al., 2005) which provides aerosol extinction measurements (e.g. Vanhellemont et al.,

2008) that can be directly compared with those retrieved from MAESTRO observations. MAESTRO is currently the only satellite instrument capable of simultaneously measuring vertical profiles of both water vapour and extinction by fine aerosols (Sioris et al., 2010b) down to the mid-troposphere. The MAESTRO water vapour retrieval relies on the 940 nm absorption band and is described by Sioris et al. (2010a) and updated recently (Sioris et al., 2015). The water vapour profiles have ~1 km vertical resolution (Sioris et al., 2010). Figures 1-2 present the validation of MAESTRO water vapour. MAESTRO is seen to have less scatter than ACE-FTS below 6.5 km. Between 6.5 and 19.5 km, the median of the relative differences between MAESTRO and ACE-FTS of their individual collocated profiles is < 20%, which is also true only for MIPAS IMK data (Stiller et al., 2012) considering the other UTLS water vapour data products compared in Fig. 2. However, due to the relatively large noise in the MAESTRO lower stratospheric water vapour data (Fig. 2), the scatter in the relative differences between individual coincident ACE-FTS and MAESTRO profiles of is on the order of ~35%, whereas those between ACE-FTS and other atmospheric sounders are typically on the order of ~10% in this region.

Sioris et al. (2010a) found a weak sensitivity of the water vapour retrieval to significant perturbations in aerosol extinction. As discussed in Sioris et al. (2010a), the weaker sensitivity of MAESTRO water vapour to aerosol extinction relative to other solar occultation instruments which have used this absorption band, namely Polar Ozone and Aerosol Measurement (POAM) III and SAGE II, is due to the availability of 'off' wavelengths (i.e. with minimal absorption by water vapour) on both sides of the water vapour band, which neither of these other instruments incorporated into their channel selection. This issue is also true for SAGE III (Thomason et al., 2010) with neighbouring channels at 869 and 1021 nm, but to a lesser extent than for SAGE II.

ACE-FTS gridded version 3.5 water vapour profiles are used in the study (Boone et al., 2013) and are assumed to have 3 km vertical resolution. This dataset has been validated as discussed in the companion paper. Over the microwindows used to retrieve water vapour from ACE-FTS spectra (Boone et al., 2005), absorption by this trace gas is completely uncorrelated with the spectrally smooth aerosol extinction signature. The insensitivity to aerosol extinction of water vapour retrieved from high-resolution solar occultation spectra using microwindows is well known (e.g. Rinsland et al., 1994; Michelsen et al., 2002; Steele et al., 2006; Uemera et al.,

2005). The use of a slope term in each microwindow accounts for the smooth aerosol extinction (Boone et al., 2005). Over each microwindow used to retrieve water vapour, no higher order baseline terms are necessary. The complete insensitivity to aerosol extinction is an advantage of the microwindow technique relative to the band-integrated approach used in the MAESTRO water vapour retrieval. This advantage is possible due to the high spectral resolution of ACE-FTS which assists in separating the continuum level from the deep absorption lines due to light, gas phase species such as water vapour.

The monthly tropopause height is defined by the lower of the lowest local minimum above 5 km or the lowest height above 5 km at which the lapse rate is < 2 K/km in monthly median temperatures from the Global Environmental Multiscale (GEM) regional weather forecast model (Laroche et al., 1999). Further details are given in the companion paper.

To obtain a water vapour relative anomaly time series for the UTLS, the method is described by Sioris et al. (2015)**.** The monthly climatology, used to deseasonalize the time series, is generated by averaging the monthly medians over the populated years, with a minimum sample size of 20 observations per altitude bin in each individual month. Between 5.5 and 19.5 km using 1 km vertical bins, climatological profiles are obtained for all calendar months except April, June, August, and December at northern high latitudes (60-90°N) and all months except February, June, October, and December at southern high-latitudes (60-90°S), as ACE does not sample these regions in these months. For the case studies presented next, there are at least 65 profiles measured by MAESTRO and by ACE-FTS for each month in the July-September 2011 period at southern high latitudes (Puyehue-Cordón Caulle) and for May 2010 at northern high latitudes (Eyjafjallajökull).

3 Results

3.1 Puyehue Cordón Caulle

The Puyehue-Cordón Caulle volcano (40.59°S, 72.12°W) erupted explosively in early June of 2011. The volcanic explosivity index (VEI, Newhall and Self, 1982) was 5 (http://www.volcano.si.edu/volcano.cfm?vn=357150). Figure 3 shows MAESTRO time series in the UT region, indicating an anomalous increase in water vapour mixing ratio in July 2011,

increasing relative to May 2011, whereas in a typical year, the mixing ratio can be seen to decrease from May to September as part of the strong seasonal cycle. Note that the upper troposphere is not warmer in July or August of 2011 than in May 2011 according to GEM model analysis temperatures (Laroche et al., 1999) sampled at the locations of ACE observations, and yet it is more humid. Figure 4 is a deseasonalized version of Fig. 3, illustrating a large increase in high latitude UTWV in the austral winter of 2011 that significantly biases (at the 1σ level) the inferred decadal trend at 8.5 km. In austral winter, the southern high-latitude observations occur from early July to austral spring equinox covering latitudes from 60 to 81°S with a two day absence in late August, indicating the good coverage of southern high latitudes by ACE in this season. Note that the spatiotemporal sampling repeats annually for ACE as illustrated by Randel et al. (2012). The typical 'stratospheric' monthly zonal mean values (<10 ppm) that annually appear in September at 8.5 km did not appear in September 2011 (Fig. 3).

To connect the clearly enhanced UTWV at southern high latitudes to the eruption of Puyehue-Cordón Caulle (Puyehue hereafter), UTWV profiles in the 40-60°S band, which contains the latitude of this volcano, were contrasted between July 2011 and July 2012 (a normal July). Figure 5 shows a statistically significant increase in zonal median UTWV in the 40-60°S latitude band as well for July 2011 relative to July 2012, and no significant increase above 10 km. ACE samples the 40-60°S band in the first 12 days of the month and then samples the 60-90°S band (actually 60-66°S) for the remainder of the month. The large increase in water vapour at 8 km in July 2011 is present in both latitude bands. The consistency of these ratio profiles between middle and high southern latitudes provides evidence of the poleward transport in the upper troposphere of water vapour emitted by the Puyehue eruption.

The anomalous, sharp peak in monthly median aerosol extinction in the southern high-latitude upper troposphere observed by MAESTRO (not shown) and ACE-Imager (Fig. 6) confirms Puyehue aerosol observations by other satellite instruments (Vernier et al., 2013; Theys et al., 2014) and corroborates the volcanic origin of the water vapour enhancement. The median and the mean aerosol extinction in the upper troposphere are nearly equal because the Puyehue aerosol layer has spread across all longitudes by July 2011 (Vernier et al., 2013). The southern high latitude upper troposphere can be quite cold in austral winter and local condensation is known to occur (Randel et al., 2012). However, the widespread layer in Fig. 6 is unlikely to be

due to homogeneously nucleated cirrus given that the monthly median relative humidity (RH) in July 2011 is only ~60% at the peak (Fig. 7). This RH peak is present in the July climatology (Fig. 7) but it is much more subtle, closer to the tropopause and the RH at its peak is typically half (i.e. 30%) of the July 2011 value. RH profiles (Fig. 7) are used to emphasize that most of the water emitted from the volcanic eruption will tend to remain in the vapour phase as it resides in the southern high-latitude upper troposphere. At southern mid latitudes (40-60°S), the earliest available MAESTRO observations (i.e. early July 2011) indicate a fine aerosol plume peaking at 8.5 km (not shown). Relative humidity in the 40-60°S band obtained using MAESTRO water vapour peaks at 41±14% at 8.5 km (Fig. 7), establishing that the upper troposphere in this mid-latitude band was not saturated one month after the eruption. Both the mid-latitude and high-latitude RH profiles in July 2011 peak at 8.5 km with slightly higher relative humidity at high latitudes where the volcanic UTWV enhancement encountered cooler ambient air at altitudes between 7.5 and 9.5 km.

Considering both the ACE-FTS (Bernath et al., 2005) and MAESTRO measurements, the largest relative enhancements in water vapour in July 2011 occur at 7.5-9.5 km, where a doubling is observed relative to normal mixing ratios for that month (see Fig. 8). By August 2011, the relative anomaly remains of similar magnitude throughout the upper troposphere, and is statistically significant (1σ) at 7.5-8.5 km (seen by both instruments), whereas in September 2011, the UTWV enhancement is statistically insignificant. The decrease over these winter months is consistent with the lifetime of water vapour in the upper troposphere (Ehhalt, 1973). In July 2011, relative humidity of 100% with respect to ice (see Murray, 1967) was reached in some profile observations in the southern high-latitude upper troposphere with the corresponding MAESTRO aerosol extinction observations indicating a vertically thin plume of fine particles. Thus, ice-coated tropospheric aerosols are inferred to be present for these cases.

The large enhancement in UTWV at southern high latitudes in July 2011 however does not significantly change the cooling rate at the surface (see Appendix A for details of the method).

3.2 Eyjafjallajökull

Eyjafjallajökull (63.63°N, 19.62°E) began erupting on 14 April 2010 below 210 m of glacial ice (Magnússon et al., 2012), reaching an altitude of 10 km (Gudmundsson et al., 2012). This was followed by a second eruption on 05 May 2010 that also reached ~10.0 km (Gudmundsson et al.,

2012). ACE does not cover northern high latitudes in April, but in May 2010, MAESTRO and ACE-FTS both see statistically significant enhancements in water vapour at 8.5-9.5 km (Fig. 9). In fact, at 9.5 km, the (69±10)% anomaly in May 2010 is the largest anomaly at this altitude in any of the 63 months that sample northern high latitudes in either dataset. The stated statistical significance considers the respective interannual variability for the month of May and the respective relative standard error for May 2010 for each dataset. The monthly mean tropopause height in May 2010 is 10.5 km but some individual observations have a tropopause height as high as 11.5 km**.** The peak of the Eyjafjallajökull aerosol layer is at 7.5 km approximately one month after eruption (Fig. 10). Figure 10 reveals an upper tropospheric aerosol layer that is not homogeneously spread throughout northern high latitudes based on differences between MAESTRO 560 nm May 2010 mean and median aerosol extinction profiles and the fact that both peak at 7.5 km. The ACE-Imager NIR data at northern high latitudes in May 2010 confirm an aerosol layer at 7.5±0.5 km (not shown). The Arctic oscillation would be expected to increase water vapour by < 8% at 8.5-9.5 km in May 2010 according to the regression using year-round monthly-sampled data as determined in the companion paper (Sioris et al., 2015) and is thus insufficient to explain the increase. Also, although dehydrated and rehydrated layers were observed in the 2010 winter (Khaykin et al., 2013), water vapour in the upper troposphere and lower stratosphere (UTLS, 5-20 km) in the northern high latitude region in March 2010 was normal according to both MAESTRO and ACE-FTS. ACE does not sample northern high latitudes in June. In July 2010, enhanced UTWV is observed by both instruments only at the local tropopause (11.5 km), but for MAESTRO, this enhancement is not statistically significant.

4 Discussion

In the time span of 14 months (April 2010 to June 2011), two extratropical eruptions with VEI ≥4 occurred that were followed by significantly enhanced UTWV at high latitudes in the hemisphere of the eruption. Monthly median UTWV VMR increases of up to 50% were observed. For Eyjafjallajökull, the enhancement was not significant in July 2011, three months after the initial eruption, and similarly for Puyehue, the period of significantly enhanced UTWV spanned two months. While both of these impacted the high-latitude, upper troposphere in the hemisphere of the eruption, one of the eruptions, namely Puyehue, is a southern mid-latitude volcano. Volcanic UTWV enhancements in the extratropics during the cold season are more

readily detected in monthly zonal median data because of the low background VMR of water vapour in this region and season, owing to the lack of deep convection. Secondly, reduced precipitation in the wintertime high latitude upper troposphere provides a residence time for the volcanic enhancement on the order of the timescale of the analysis. Thus, the timing and location of the Puyehue eruption were favourable for detecting its water vapour enhancement at southern high latitudes. During poleward transport, air parcels follow isentropes typically to higher altitudes. Such transport involves adiabatic cooling which can lead to saturation. However, saturation does not necessarily imply complete removal from the atmosphere or even the upper troposphere. With the rise in altitude, the ice crystals that form may fall, but they may be vaporized very quickly given their small size and the warmer temperatures below. The net effect is that an air parcel transported poleward on an upward sloping isentrope may experience little change in the vertical profile of the water vapour enhancement.

Eyjafjallajökull is likely a special case since the volcano was below > 200 m of glacial ice, some of which was vaporized in the process and rose in the eruption column. It is interesting to note that Eyjafjallajökull (Sears et al., 2013) and Puyehue (Pumphrey et al., 2015; Vernier et al., 2013) emitted relatively little SO_2 considering their VEI values, thereby reducing the probability of water uptake by the resulting sulphate aerosol. Volcanic emissions are known to be more variable in terms of SO_2 than water vapour (Pinto et al., 1989).

5 Conclusions

Due to the sporadic nature of volcanic eruptions, the UTWV variability explained by volcanic emissions at high latitudes over a decade is much less than is attributable to the annular mode of internal variability. However, this study shows that volcanic emissions can lead to UTWV increases on a monthly timescale of >50%, comparable to the UTWV increases observed during the largest annular mode negative events (Sioris et al., 2015).

While the climatic impact of enhanced water vapour due to the Puyehue eruption is shown to be minor, particularly given the short period of this volcanic enhancement, such increases are relevant for UTWV trend studies, particularly if an eruption occurs near the start or end of the period under consideration.

Finally, MAESTRO, a solar occultation instrument operating visible and near-infrared wavelengths, has the unique capability among current space-borne instruments to simultaneously observe vertical profiles of aerosol extinction and water vapour in the UTLS to provide an understanding of the impact of volcanic emissions on the water vapour budget and trends in water vapour.

Appendix A: Cooling rate differences

In order to investigate the impact on volcanic UTWV enhancements on surface temperature, cooling rate vertical profiles are calculated for July 2011 using MODTRAN5.2 (e.g. Bernstein et al., 1996) assuming an Antarctic surface altitude of 2.5 km, the tropospheric monthly median profile of the GEM analysis temperatures (to the surface), aerosol extinction profiles from MAESTRO at 560 nm down to 5 km and two water vapour cases:

1) using MAESTRO July climatological median water vapour between 6.5 and 9.5 km, and

2) with the increase in water vapour over this altitude range due to the Puyehue eruption determined by multiple linear regression with the Antarctic oscillation index (Mo, 2000) (http://www.cpc.ncep.noaa.gov/products/precip/CWlink/) plus a constant being the other basis functions. A monthly timestep is used with the Puyehue eruption basis function having a value of 1 for July-August 2011 and 0 in all other months for the purpose of the regression analysis.

The use of a multiple linear regression adjusts for a minor contribution by the Antarctic oscillation to the July 2011 UTWV enhancement.

Acknowledgements

The ACE mission is supported primarily by the Canadian Space Agency. David Plummer (Environment Canada) is acknowledged for his encouragement to perform cooling rate simulations for the Puyehue eruption. We appreciate the availability of the AO and AAO indices from the National Oceanic and Atmospheric Administration.

References

Bernath, P. F., McElroy, C. T., Abrams, M. C., Boone, C. D., Butler, M., Camy-Peyret, C., Carleer, M., Clerbaux, C., Coheur, P.-F., Colin, R., DeCola, P., DeMazière, M., Drummond, J.

R., Dufour, D., Evans, W. F. J., Fast, H., Fussen, D., Gilbert, K., Jennings, D. E., Llewellyn, E. J., Lowe, R. P., Mahieu, E., McConnell, J. C., McHugh, M., McLeod, S. D., Michaud, R., Midwinter, C., Nassar, R., Nichitiu, F., Nowlan, C., Rinsland, C. P., Rochon, Y. J., Rowlands, N., Semeniuk, K., Simon, P., Skelton, R., Sloan, J. J., Soucy, M.-A., Strong, K., Tremblay, P., Turnbull, D., Walker, K. A., Walkty, I., Wardle, D. A., Wehrle, V., Zander, R., and Zou, J.: Atmospheric Chemistry Experiment (ACE): mission overview, Geophys. Res. Lett., 32, L15S01, doi:10.1029/2005GL022386, 2005.

Bernstein, L. S., Berk, A., Acharya, P. K., Robertson, D. C., Anderson, G. P., Chetwynd, J. H., and Kimball, L. M.: Very narrow band model calculations of atmospheric fluxes and cooling rates, J. Atmos. Sci., 53, 2887-2904, 1996.

Boone, C. D., Walker K. A., and Bernath, P. F.: Version 3 retrievals for the Atmospheric Chemistry Experiment Fourier Transform Spectrometer (ACE-FTS). The Atmospheric Chemistry Experiment ACE at 10: A Solar Occultation Anthology, Peter F. Bernath, A. Deepak Publishing, Hampton, VA, USA, 2013.

Boone, C. D., Nassar, R., Walker, K. A., Rochon, Y., McLeod, S. D., Rinsland, C. P., and Bernath, P. F.: Retrievals for the atmospheric chemistry experiment Fourier-transform spectrometer, Appl. Opt., 44, 7218-7231, 2005.

Bourassa, A. E., Robock, A., Randel, W. J., Deshler, T., Rieger, L. A., Lloyd, N. D., Llewellyn, E. J., and Degenstein, D. A.: Large volcanic aerosol load in the stratosphere linked to Asian monsoon transport, Science, 337, 78-81, 2012.

Brasseur, G. P., Cox, R. A., Hauglustaine, D., Isaksen, I., Lelieveld, J., Lister, D. H., Sausen, R., Schumann, U., Wahner, A., and Wiesen, P.: European Scientific Assessment of the atmospheric effects of aircraft emissions, Atmos. Env., 32, 2329-2418, 1998.

Ehhalt, D. H.: Turnover times of ^{137}Cs and HTO in the troposphere and removal rates of natural aerosol particles and water vapour, J. Geophys. Res., 78, 7076-7086, 1973.

Gudmundsson, M. T., Thordarson, T., Höskuldsson, Á., Larsen, G., Björnsson, H., Prata, F. J., Oddsson, B., Magnússon, E., Högnadóttir, T., Petersen, G. N., Hayward, C. L., Stevenson, J. A., and Jónsdóttir, I.: Ash generation and distribution from the April-May 2010 eruption of Eyjafjallajökull, Iceland, Sci. Rep. 2, 572; doi:10.1038/srep00572, 2012.

Hartmann, D. L., Klein Tank, A. M. G., Rusticucci, M., Alexander, L.V., Brönnimann, S., Charabi, Y., Dentener, F. J., Dlugokencky, E. J., Easterling, D. R., Kaplan, A., Soden, B. J., Thorne, P. W., Wild M., and Zhai, P.M.: Observations: Atmosphere and Surface. In: Climate Change 2013: The Physical Science Basis. Contribution of Working Group I to the Fifth Assessment Report of the Intergovernmental Panel on Climate Change [Stocker, T.F., D. Qin, G.-K. Plattner, M. Tignor, S.K. Allen, J. Boschung, A. Nauels, Y. Xia, V. Bex and P.M. Midgley (eds.)]. Cambridge University Press, Cambridge, United Kingdom and New York, NY, USA, 2013.

Junge, C. E.: Air chemistry and radioactivity, Academic Press, New York, 1963.

Khaykin S. M., Engel, I., Vömel, H., Formanyuk, I. M., Kivi, R., Korshunov, L. I., Krämer, M., Lykov, A. D., Meier, S., Naebert, T., Pitts, M. C., Santee, M. L., Spelten, N., Wienhold, F. G., Yushkov, V. A., and Peter, T.: Arctic stratospheric dehydration – Part 1: Unprecedented observation of vertical redistribution of water. Atmos. Chem. Phys., 13, 11503–11517, 2013.

Laroche, S., Gauthier, P., St-James, J., and Morneau, J.: Implementation of a 3D variational data assimilation system at the Canadian Meteorological Centre. Part II: The regional analysis. Atmos. Ocean, 37, 281–307, 1999.

Magnússon, E., Gudmundsson, M. T., Roberts, M. J., Sigurðsson, G., Höskuldsson, F., and Oddsson, B.: Ice-volcano interactions during the 2010 Eyjafjallajökull eruption, as revealed by airborne imaging radar, J. Geophys. Res., 117, B07405, doi: 10.1029/2012JB009250, 2012.

McElroy, C. T., Nowlan, C. R., Drummond, J. R., Bernath, P. F., Barton, D. V., Dufour, D. G., Midwinter, C., Hall, R. B., Ogyu, A., Ullberg, A., Wardle, D. I., Kar, J., Zou, J., Nichitiu, F., Boone, C. D., Walker, K. A., and Rowlands, N.: The ACE-MAESTRO instrument on SCISAT: description, performance, and preliminary results. Appl. Opt. 46, 4341–4356, 2007.

Michelsen, H. A., Manney, G. L., Irion, F. W., Toon, G. C., Gunson, M. R., Rinsland, C. P., Zander, R., Mahieu, E., Newchurch, M. J., Purcell, P. N., Remsberg, E. E., Russell III, J. M., Pumphrey, H. C., Waters, J. W., Bevilacqua, R. M., Kelly, K. K., Hintsa, E. J., Weinstock, E. M., Chiou, E.-W., Chu, W. P., McCormick, M. P., and Webster, C. R.: ATMOS version 3 water vapor measurements: Comparisons with observations from two ER-2 Lyman-a hygrometers,

MkIV, HALOE, SAGE II, MAS, and MLS, J. Geophys. Res., 107, 4027, 10.1029/2001JD000587, 2002.

Mo, K. C.: Relationships between low-frequency variability in the southern hemisphere and sea surface temperature anomalies. J. Climate, 13, 3599-3610, 2000.

Murray, F. W.: On the computation of saturation vapor pressure, J. Appl. Meteorol., 6, 203-204, 1967.

Newhall, C. G., and Self, S.: The Volcanic Explosivity Index (VEI): An estimate of explosive magnitude for historical volcanism, J. Geophys. Res. 1231-1238, 1982.

Pinto, J. P., Turco, R. P., and Toon, O. B.: Self-limiting physical and chemical effects in volcanic eruption clouds, J. Geophys. Res., 94, 11165-11174, 1989.

Prospero, J. M., Charlson, R. J., Mohnen, V., Jaenicke, R., Delany, C., Moyer, J., Zoller, W., and Rahn, K.: The atmospheric aerosol system: An overview, Rev. Geophys., 21, 1607-1629, 1983.

Pruppacher, H. R., and Klett, J. D.: Microphysics of clouds and precipitation, Springer, New York, 2010.

Pumphrey, H. C., Read, W. G., Livesey, N. J., and Yang, K.: Observations of volcanic SO_2 from MLS on Aura, Atmos. Meas. Tech., 8, 195–209, 2015.

Randel, W. J., Moyer, E., Park, M., Jensen, E., Bernath, P., Walker, K., and Boone, C.: Global variations of HDO and HDO/H_2O ratios in the upper troposphere and lower stratosphere derived from ACE-FTS satellite measurements, J. Geophys. Res., 117, D06303, doi:10.1029/2011JD016632, 2012.

Rinsland, C. P., Gunson, M. R., Abrams, M. C., Lowes, L. L., Zander, R., Mahieu, E., Goldman, A., Ko, M. K. W., Rodriguez, J. M., and Sze, N. D.: Heterogeneous conversion of N_2O_5 to HNO_3 in the post-Mount Pinatubo eruption stratosphere, J. Geophys. Res., 99, 8213-8219, 1994a.

Sears, T. M., Thomas, G. E., Carboni, E., Smith, A. J. A., and Grainger, R. G.: SO_2 as a possible proxy for volcanic ash in aviation hazard avoidance, J. Geophys. Res. Atmos., 118, 5698–5709, doi:10.1002/jgrd.50505, 2013.

Sioris, C. E., Zou, J., McElroy, C. T., McLinden, C. A., and Vömel, H., High vertical resolution water vapour profiles in the upper troposphere and lower stratosphere retrieved from MAESTRO solar occultation spectra. Adv. Space. Res., 46, 642–650, 2010a.

Sioris, C. E., Boone, C. D., Bernath, P. F., Zou, J., McElroy, C. T., McLinden, C. A.: ACE observations of aerosol in the upper troposphere and lower stratosphere from the Kasatochi volcanic eruption, J. Geophys. Res., 115, D00L14, doi:10.1029/2009JD013469, 2010b.

Sioris, C. E., Zou, J., Plummer, D. A., Boone, C. D., McElroy, C. T., Sheese, P. E., Moeini, O., and Bernath, P. F.: Upper tropospheric water vapour variability at high latitudes - Part 1: Influence of the annular modes, Atmos. Chem. Phys. Discuss., 15, 22291-22329, 2015.

Soden, B. J., Wetherald, R. T., Stenchikov, G. L., and Robock, A.: Global cooling after the eruption of Mount Pinatubo: A test of climate feedback by water vapor, Science, 296, 727-730, 2002.

Solomon, S., Rosenlof, K. H., Portmann, R. W., Daniel, J. S., Davis, S. M., Sanford, T. J., and Plattner, G.-K.: Contributions of stratospheric water vapor to decadal changes in the rate of global warming, Science, 327, 1219-1223, doi: 10.1126/science.1182488, 2010.

Steele, H. M., Eldering, A., and Lumpe, J. D.: Simulations of the accuracy in retrieving stratospheric aerosol effective radius, composition, and loading from infrared spectral transmission measurements, Appl. Opt., 45, 2014-2027, 2006.

Stiller, G. P., Kiefer, M., Eckert, E., von Clarmann, T., Kellmann, S., García-Comas, M., Funke, B., Leblanc, T., Fetzer, E., Froidevaux, L., Gomez, M., Hall, E., Hurst, D., Jordan, A., Kämpfer, N., Lambert, A., McDermid, I. S., McGee, T., Miloshevich, L., Nedoluha, G., Read, W., Schneider, M., Schwartz, M., Straub, C., Toon, G., Twigg, L.W., Walker, K. and Whiteman, D. N.: Validation of MIPAS IMK/IAA temperature, water vapor, and ozone profiles with MOHAVE-2009 campaign measurements, Atmos. Meas. Tech., 5, 289–320, 2012.

Theys, N., De Smedt, I., Van Roozendael, M., Froidevaux, L., Clarisse, L., and Hendrick, F.: First satellite detection of volcanic OClO after the eruption of Puyehue-Cordón Caulle, Geophys. Res. Lett., 41, 667–672, doi:10.1002/2013GL058416, 2014.

Thomason, L.W., Moore, J. R., Pitts, M. C., Zawodny, J. M., and Chiou, E.W.: An evaluation of the SAGE III version 4 aerosol extinction coefficient and water vapor data products, Atmos. Chem. Phys., 10, 2159–2173, 2010.

Uemera, N., Kuriki, S., Nobuta, K., Yokota, T., Nakajima, H., Sugita, T., and Sasano, Y.: Retrieval of trace gases from aerosol-influenced infrared transmission spectra observed by low-spectral-resolution Fourier-transform spectrometers, Appl. Opt., 44, 455-466, 2005.

Vanhellemont, F., Tetard, C., Bourassa, A., Fromm, M., Dodion, J., Fussen, D., Brogniez, C., Degenstein, D., Gilbert, K. L., Turnbull, D. N., Bernath, P., Boone, C., and Walker, K. A.: Aerosol extinction profiles at 525 nm and 1020 nm derived from ACE imager data: comparisons with GOMOS, SAGE II, SAGE III, POAM III, and OSIRIS, Atmos. Chem. Phys., 8, 2027–2037, 2008.

Vernier, J-P., Fairlie, T. D., Murray, J. J., Tupper, A., Trepte, C., Winker, D., Pelon, J., Garnier, A., Jumelet, J., Pavalonis, M., Omar, A. H., and Powell, K. A.: An advanced system to monitor the 3D structure of diffuse volcanic ash clouds, J. Appl. Meteor. Climatol., 52, 2125-2138, 2013.

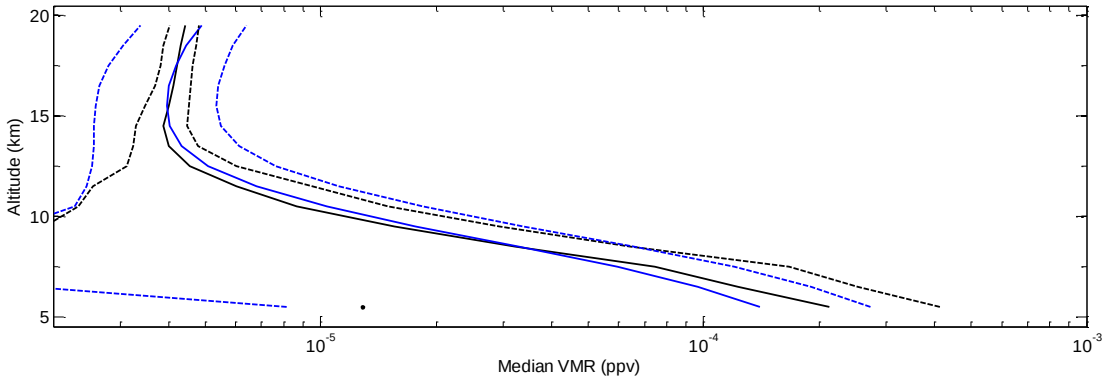

Figure 1. Comparison of global median water vapour VMRs from MAESTRO (blue) and ACE-FTS (black) (N=15000). The solid lines are the median profiles while the dashed lines bracket ±1.48 median absolute deviations (MAD) about the median.

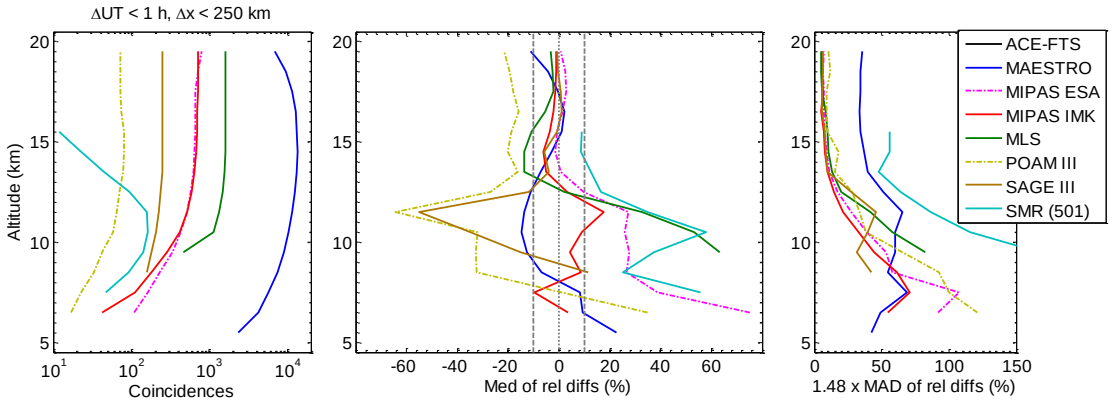

Figure 2. (left) Number of coincidences globally as a function of altitude between ACE-FTS and various limb sounders that measured water vapour in the ACE time period. The coincidence criteria are < 1 hour in time and within 250 km. (centre) Median of relative differences in water vapour versus ACE-FTS (the minuend). The profiles from the instrument with the coarser vertical resolution are smoothed to account for the difference in resolution between ACE-FTS and the correlative instrument. ACE-FTS has coarser vertical resolution than most of the chosen instruments. (right) Variability of the relative differences. SAGE is the Stratospheric Aerosol and Gas Experiment. MIPAS IMK is the Michelson Interferometer for Passive Atmospheric Sounding water vapour product developed at the Institut für Meteorologie und Klimaforschung (IMK). The MIPAS water vapour product from the European Space Agency (ESA) is also illustrated. SMR is the sub-mm radiometer on Odin and Aura MLS (Microwave Limb Sounder) is used.

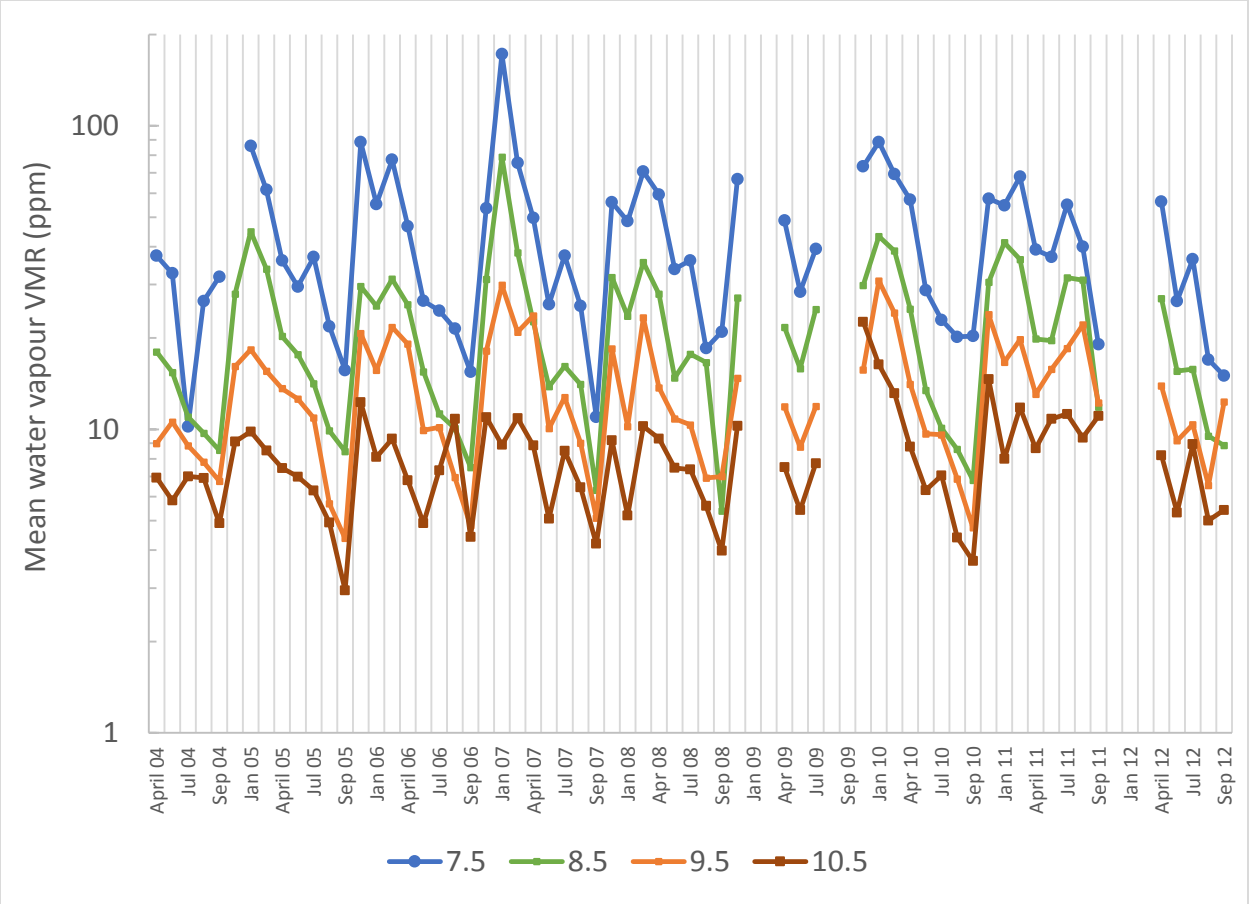

Figure 3. Monthly mean time series of MAESTRO water vapour mixing ratio at different heights (indicated in legend, in km) in the southern high-latitude tropopause region. Months of February, June, October, December are not included as ACE does not sample in this region during those months. Discontinuities indicate insufficient data during the other eight calendar months. A logarithmic scale is used for the y-axis.

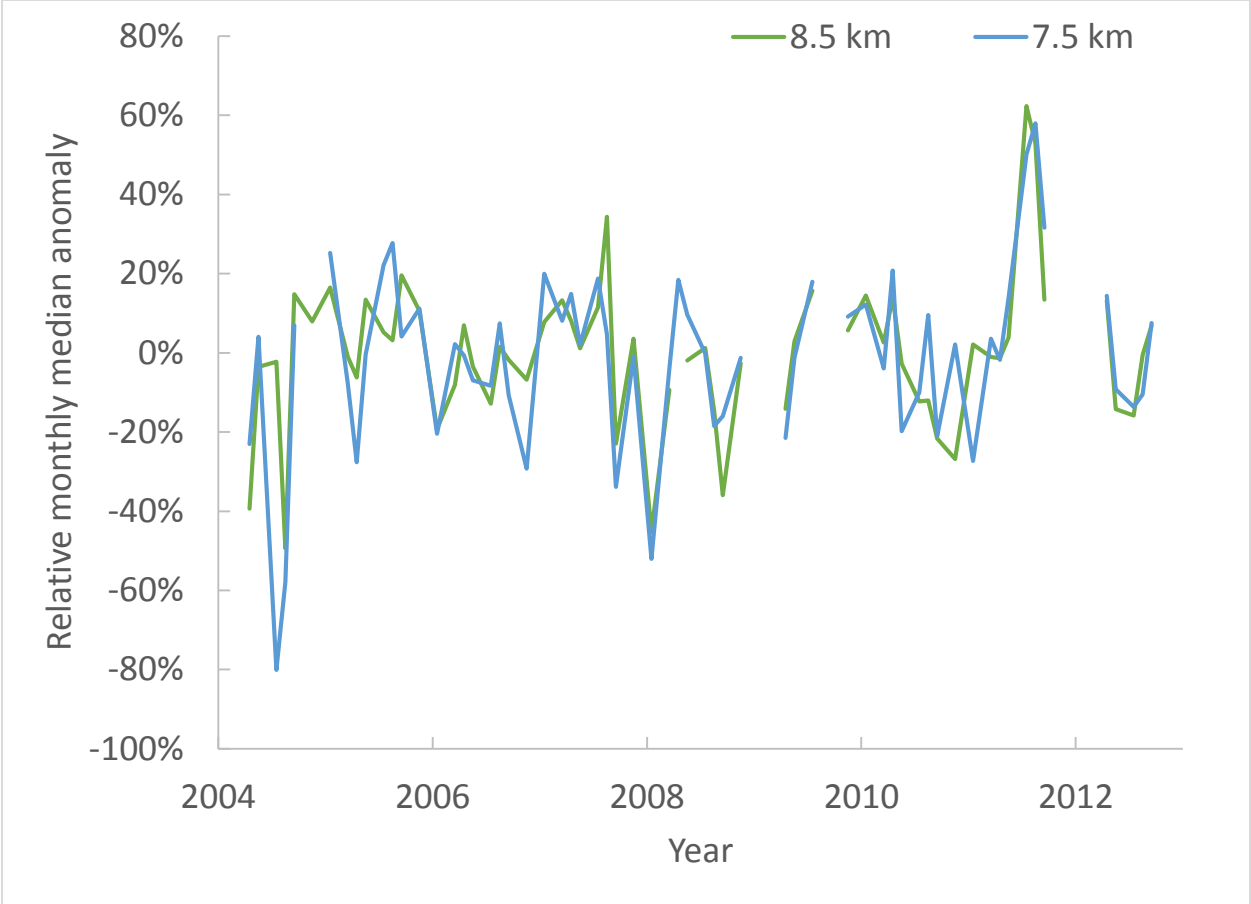

Figure 4. MAESTRO relative monthly median water vapour anomalies at 7.5 and 8.5 km at southern high-latitudes (60-90°S).

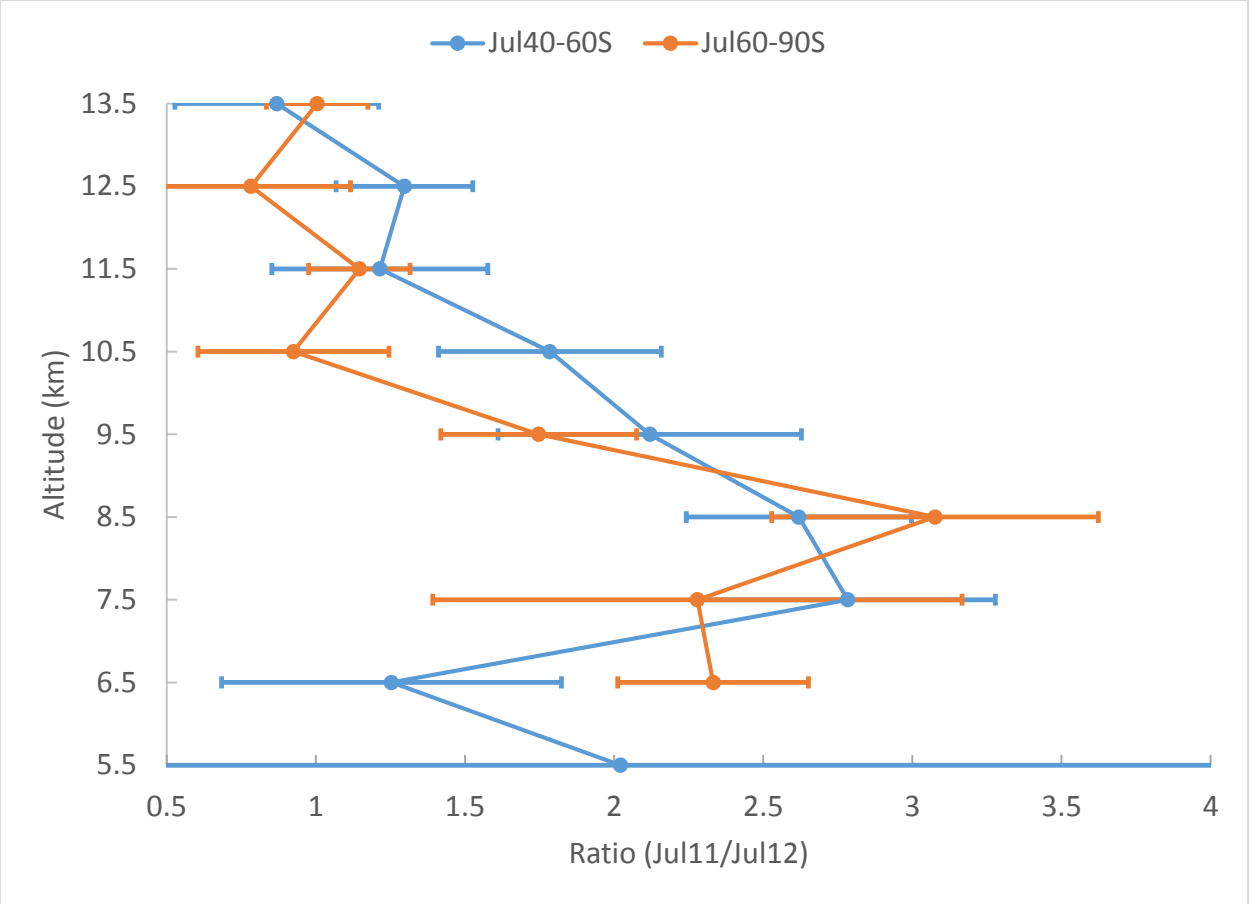

Figure 5. Enhancement factor for water vapour mixing ratio in July 2011 in the 40-60°S band (July 1-July 12, N=78) and the 60-66°S band (July 13-July 31, N=181), relative to July 2012. The error bar on the ratio profiles account for 1 standard error of the MAESTRO monthly mean for both years, combined in quadrature.

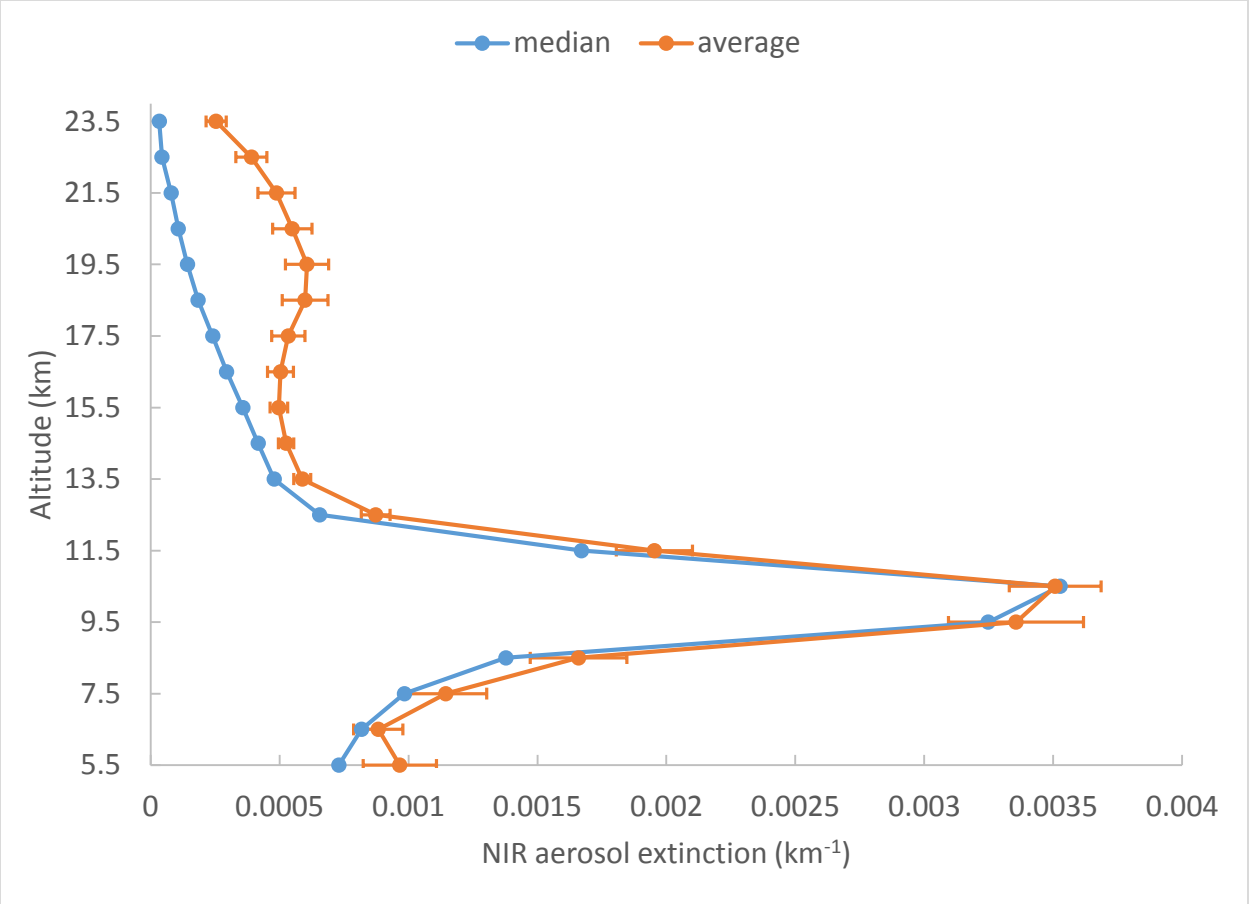

Figure 6. ACE-Imager median and average near-infrared (NIR, 1.02 μm) aerosol extinction profiles for July 2011 at southern high latitudes (N=163). The small differences between median and average extinction near the peak indicate a widespread layer in the tropopause region. One standard error of the monthly mean is shown as the error bar.

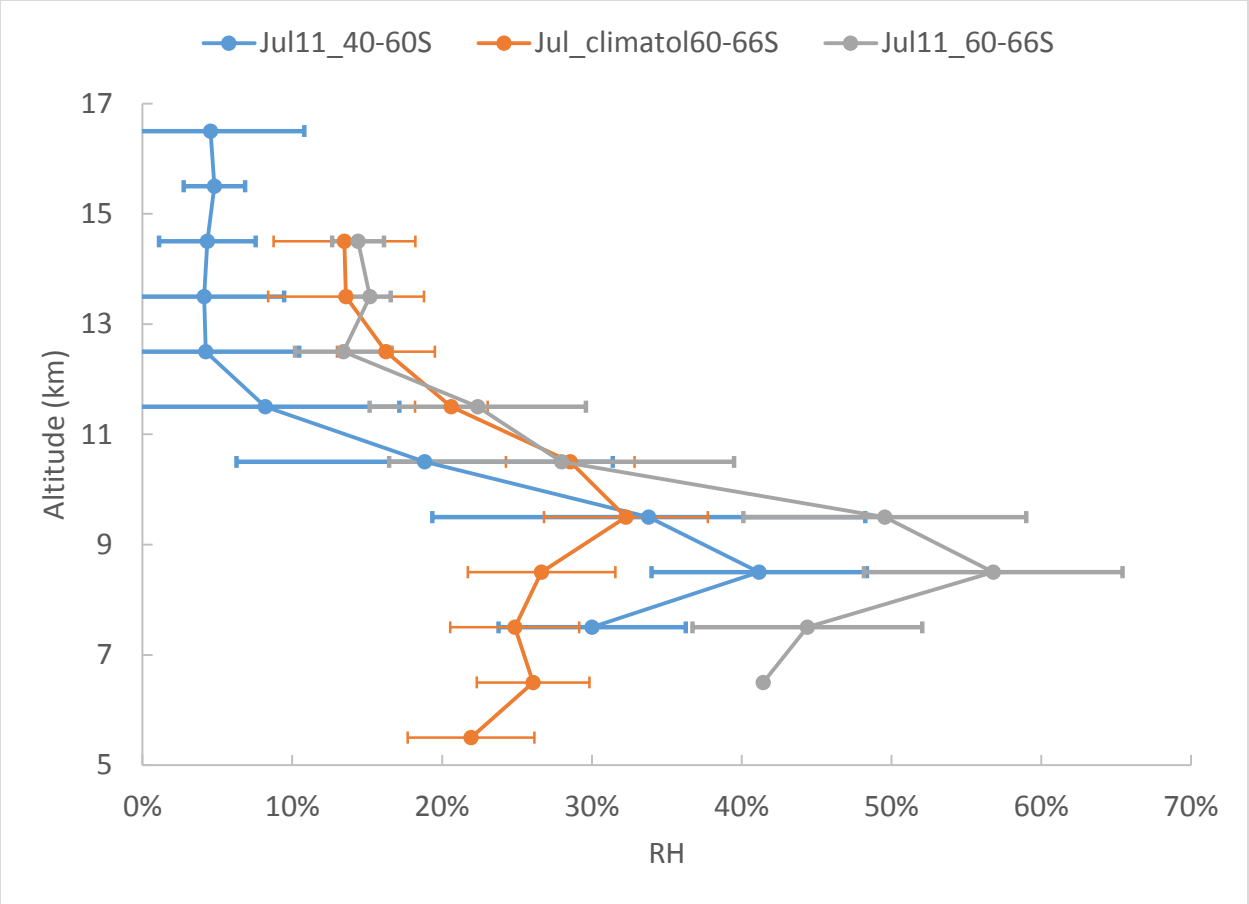

Figure 7. Relative humidity for July 2011 (40-60°S, N=52) and (60-66°S, N=111) and climatology (60-66°S, July for every year, except 2011 between 6.5 and 9.5 km, N=865) determined from MAESTRO water vapour and co-located GEM analysis temperature and pressure (Laroche et al., 1999). The uncertainty on the climatologic RH accounts for interannual variability in water vapour and saturated water vapour mixing ratio, combined in quadrature. The error bars on the July 2011 RH profiles only account for the standard error of the monthly mean water vapour.

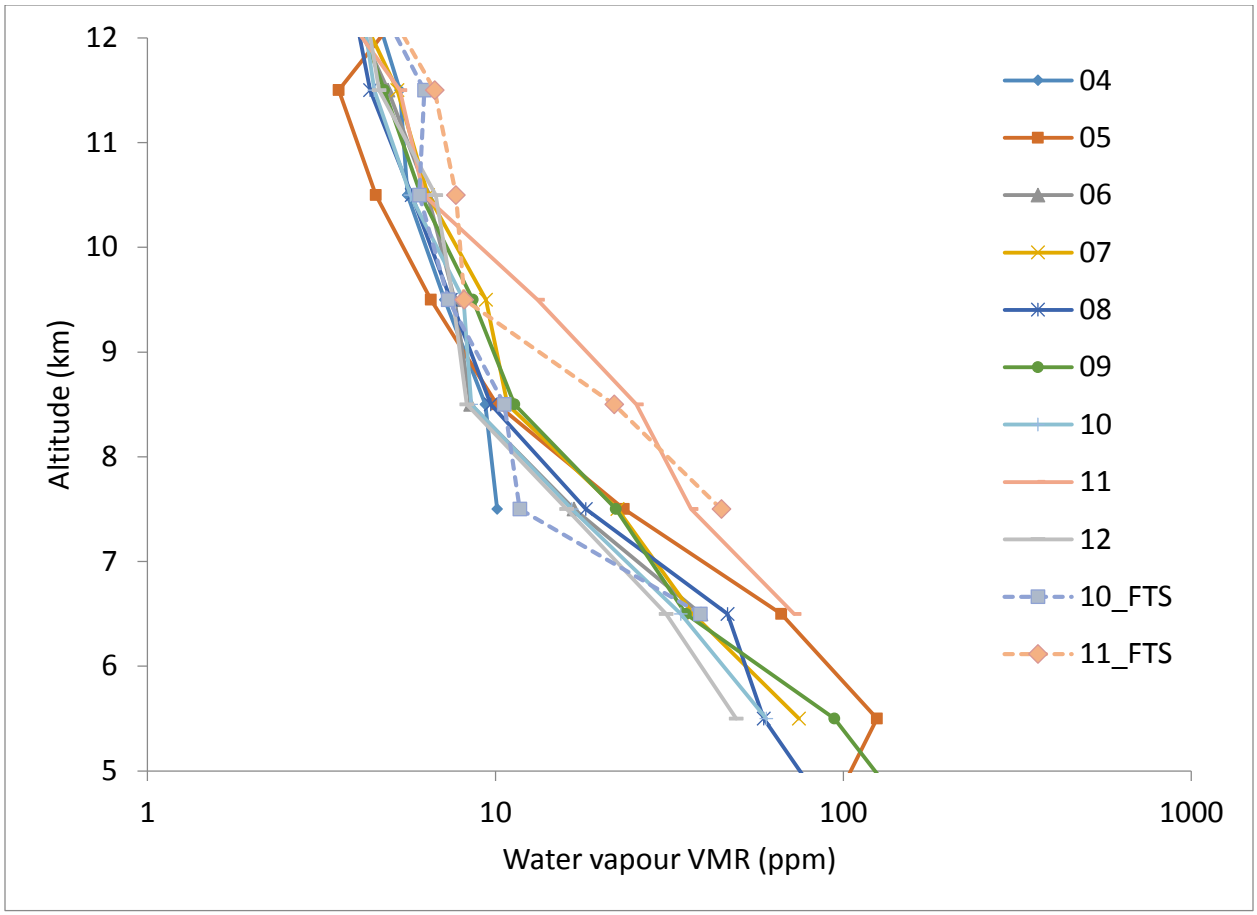

Figure 8. Southern high-latitude (60-90°S) monthly median water vapour profiles in July for different years, MAESTRO: 2004-2012, ACE-FTS: 2010 (N=169) and 2011 (N=176). A logarithmic scale is used for the x-axis. The number of July profiles (60-90°S) for MAESTRO is 96 per year on average.

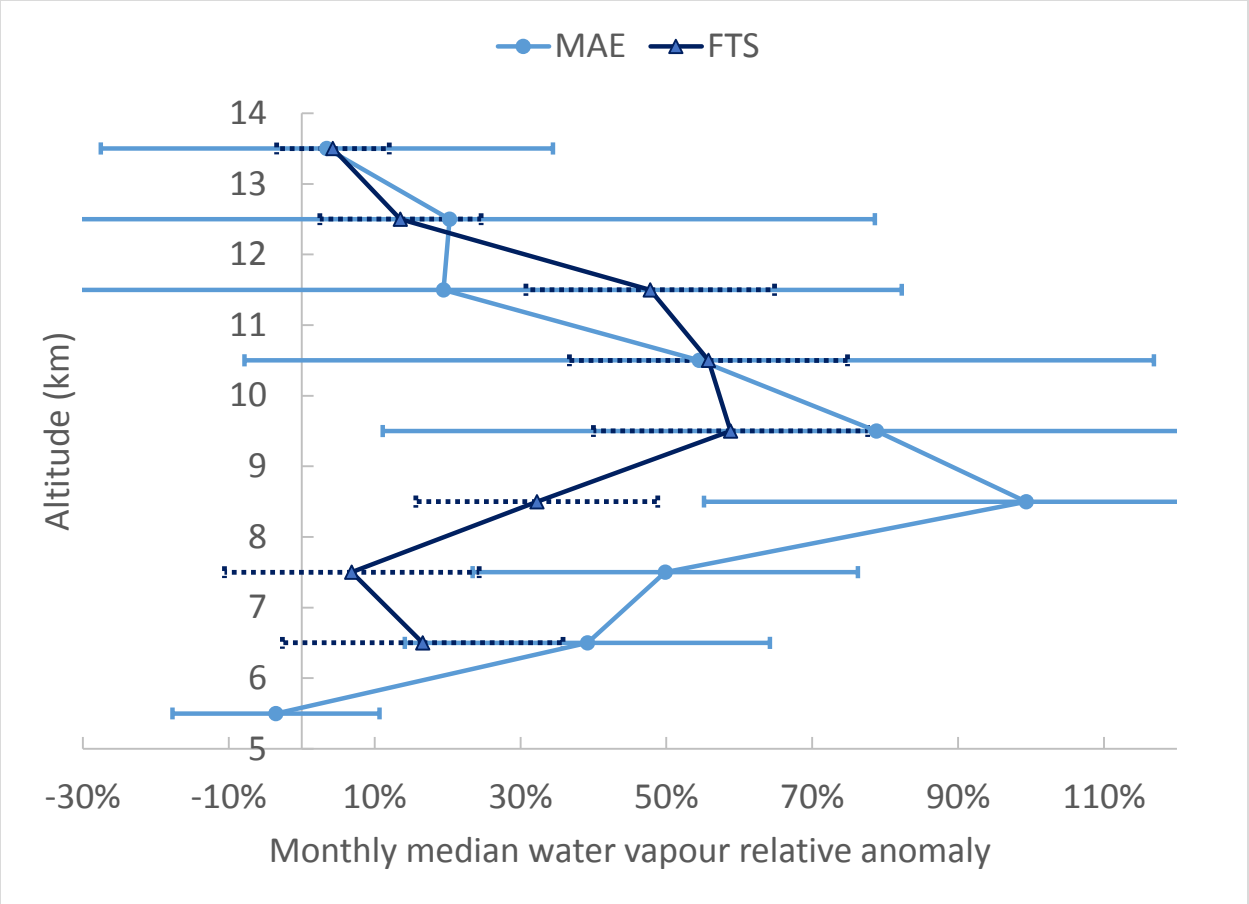

Figure 9. Water vapour relative anomaly in May 2010 at northern high latitudes following the Eyjafjallajökull eruption. The uncertainty accounts for the interannual standard deviation for May (2005-2012) and the relative standard error of individual profiles from the month of May 2010, combined in quadrature (N = 132, 178 for MAESTRO and ACE-FTS, respectively).

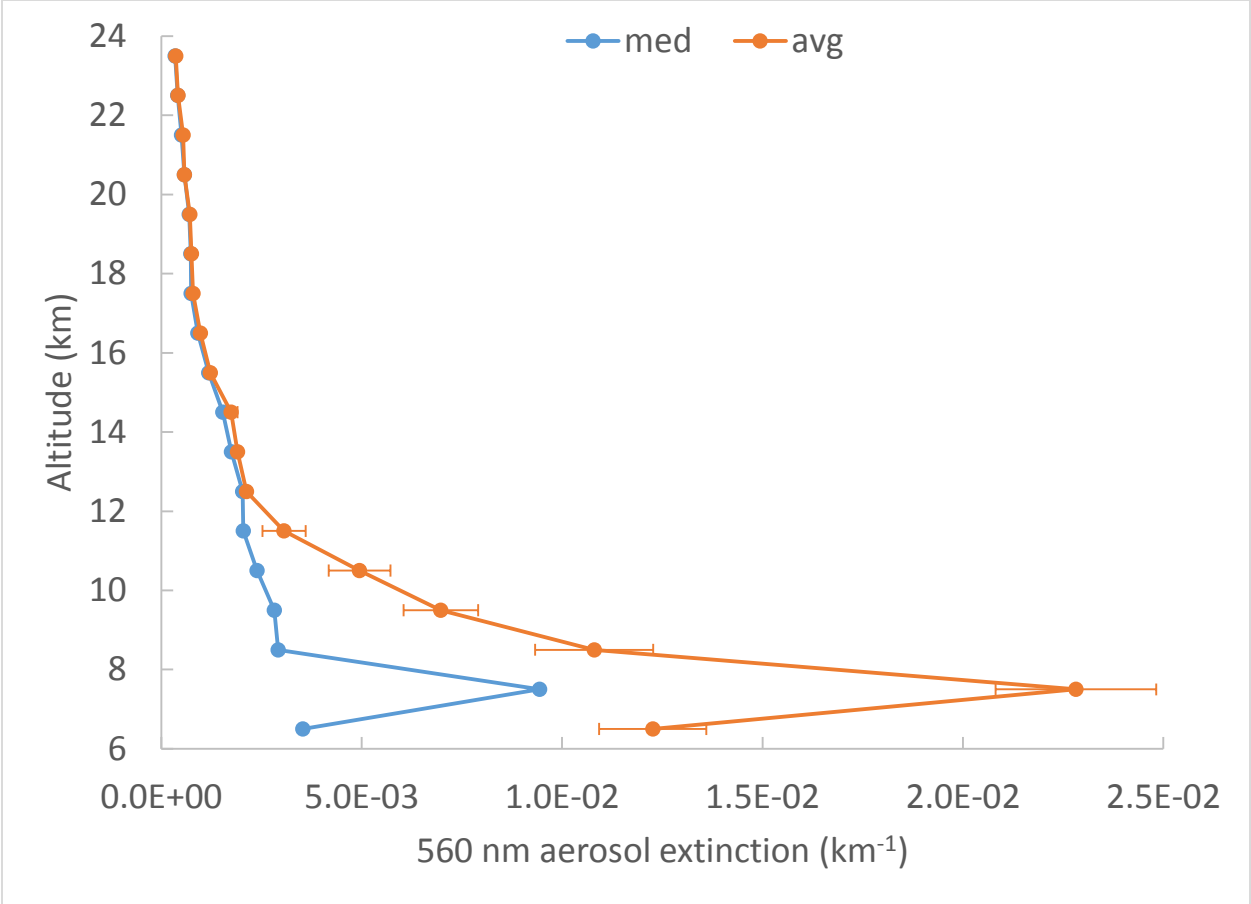

Figure 10. Median and average aerosol extinction observed by MAESTRO at 560 nm in May 2010 at northern high latitudes (N=167).